

02

Spectral-luminescent properties of glasses of the $(Y_{1-x}Yb_x)_2O_3-Al_2O_3-B_2O_3-SiO_2 + Cr_2O_3 + Na_2O$ system

© G.E. Malashkevich¹, V.V. Kouhar¹, A.A. Ramanenka¹, I.I. Azarko², V.N. Sigaev³, N.V. Golubev³, M.Z. Ziyatdinova³, E.S. Ignatieva³, S.A. Bahramov⁴

¹ Belarussian State University, Minsk, Belarus

² Stepanov Institute of Physics, Belarusian Academy of Sciences, Minsk, Belarus

³ Mendeleev University of Chemical Technology, Moscow, Russia

⁴ Arifov Institute of Ion-Plasma and Laser Technologies, Uzbekistan Academy of Sciences, 100125 Tashkent, Uzbekistan

e-mail: g.malashkevich@ifanbel.bas-net.by

Received August 03, 2021

Revised August 03, 2021

Accepted August 17, 2021

Fused yttrium-alumoborate glasses doped with ytterbium, silicon, chromium, and sodium were synthesized. The influence of the matrix on the "spectroscopic behavior" of chromium ions and the efficiency of their sensitization of Yb^{3+} luminescence was established by spectral-luminescence and EPR studies. It was found that (1) chromium in alkali-free glasses is mainly in the oxidation degree Cr(III) with an appreciable admixture of Cr(IV) and Cr(V), (2) the partial replacement of Al_2O_3 or B_2O_3 by SiO_2 and Y_2O_3 by Yb_2O_3 affects to a different extent the relative concentration of optical centers of chromium ions, (3) the addition of alkali results in the formation of Cr(VI) centers as a result of oxidation of less charged chromium ions and predominantly tetracoordinated Cr^{4+} and Cr^{5+} , (4) Cr^{3+} ions make the main contribution to the luminescence sensitization of Yb^{3+} ions, while Cr^{4+} ions and to a lesser extent Cr^{5+} play the role of luminescence quencher and internal filter. Sensitization of Yb^{3+} luminescence through the charge transfer band in Cr(VI) was found. An alkaline glass doped with Cr and Yb upon excitation through the sensitizer produced a luminescence quantum yield of 32% and the conditions for its enhancement were considered. It is shown that the temperature quenching of luminescence of Cr–Yb-containing glasses is significantly lower than that of Cr-containing glasses.

Keywords: EPR spectra, chromium and ytterbium ions, quantum yield of luminescence, sensitization and quenching of luminescence.

DOI: 10.21883/EOS.2022.01.53005.28-21

Introduction

Glasses coactivated with Cr^{3+} and Ln^{3+} ions have been intensively studied since the early 1980s, when it was proposed to use them as luminescent concentrators of solar radiation [1], and found a significant increasing of the generation efficiency of lamp-pumped erbium lasers on Yb–Er-containing glasses with additional co-activation by Cr^{3+} ions [2–4]. Although with the appearance of semiconductor sources of selective pumping the interest in using the latter to sensitise the luminescence of „laser“ ions has drastically dropped, the intensity of studies of Cr- and Cr–Ln-containing optical materials practically did not change. We see the reason for this situation in the high „spectroscopic potential“ of chromium ions, due to the possibility of a significant effect of the composition, structure and conditions of matrix synthesis on the charge state of these ions and their spectra [5–10], in an effort to obtain tunable generation on them, as well as a combination of wide absorption bands in the UV and visible regions of the spectrum and luminescence in the red and near-IR regions, which is promising for solar-pumped lasers [11] and the above specified luminescent

concentrators. A particular interest, in our opinion, belongs to the study of the nature of chromium optical centers and the processes of sensitization of the luminescence of Ln^{3+} ions by them in yttrium-aluminoborate glasses with a composition close to the huntite stoichiometry, which ensure the minimum distance between rare-earth ions $\approx 6.7 \text{ \AA}$ [12], which contributes to a reduced concentration quenching of their luminescence and a radical weakening of cooperative interactions. In particular, recently [13] it was found that the quantum yield of the luminescence of Yb^{3+} ions in such glasses, not subjected to forced dehydration, is $\approx 80\%$ at Yb_2O_3 concentration equal to 0.5 mol% and decreases to $\approx 60\%$ as the latter increases to 2 mol%. Considering the possibility of chromium ions stabilization in quartz glasses in Cr^{5+} state, which exhibits sufficiently intense broadband luminescence in the red region of the spectrum [9,10,14,15], in the present paper the task was to investigate the effect of additional introduction of silica and alkaline oxides on the spectral-luminescent properties of huntite-like glasses co-activated with chromium and ytterbium ions.

Table 1. Compositions of synthesized glasses, their density, refractive index and peak absorption coefficient of impurity OH⁻-groups

Sample	Y ₂ O ₃	Yb ₂ O ₃	Al ₂ O ₃	B ₂ O ₃	SiO ₂	Cr ₂ O ₃	Na ₂ O	ρ , g/cm ³	n	k_{OH} , cm ⁻¹
	mol%					mass%				
1	10.0	—	30.0	60.0	—	0.2	—	2.82(3)	1.61(0)	1.30
2	10.0	—	25.0	60.0	5.0	0.1	—	2.774	1.5999	2.38
3	10.0	—	25.0	60.0	5.0	0.2	—	2.768	1.6020	1.74
4	10.0	—	25.0	60.0	5.0	0.2	2.0	2.718	1.5875	1.95
5	10.0	—	25.0	60.0	5.0	0.2	4.0	2.697	1.5761	2.42
6	9.0	1.0	30.0	60.0	—	0.2	—	2.88(8)	1.60(5)	1.42
7	9.0	1.0	25.0	60.0	5.0	0.2	—	2.826	1.5982	1.49
8	8.0	2.0	30.0	60.0	—	0.2	—	2.93(5)	1.60(6)	1.42
9	8.0	2.0	25.0	60.0	5.0	0.1	—	2.872	1.5993	1.60
10	8.0	2.0	30.0	55.0	5.0	0.2	—	2.919	1.6043	2.47
11	8.0	2.0	30.0	50.0	10.0	0.2	—	2.94(2)	1.60(8)	2.41
12	8.0	2.0	30.0	45.0	15.0	0.2	—	2.964	1.6107	2.47
13	8.0	2.0	25.0	60.0	5.0	0.2	2.0	2.823	1.5863	2.53
14	8.0	2.0	25.0	60.0	5.0	0.2	4.0	2.780	1.5752	2.91
15	8.0	2.0	25.0	60.0	5.0	0.2	8.0	2.821	1.5617	2.72

Experiment

The studied glasses were synthesized by charge melting in a laboratory resistance furnace with SiC heaters in a platinum crucible at $T \approx 1480^\circ\text{C}$ in air for 60 min. As initial components Y₂O₃ (extra pure), Al(OH)₃ (pure for analysis), H₃BO₃, Yb₂O₃ (extra pure), amorphous SiO₂ (extra pure), Cr₂O₃ (chem. pure), Na₂CO₃ (chem. pure) were used. The density of the synthesized glasses (ρ) was determined by hydrostatic weighing, the refractive index (n) was measured on an Abbe NAR-3T refractometer at $\lambda = 589.3$ nm, and the relative concentration of impurity OH⁻-groups was estimated from the peak value of the absorption coefficient in the region of the main vibration of the O–H (k_{OH}) bond, which was determined by the method in [13]. These parameters and compositions (according to charge) of the synthesized glasses are summarized in the Table 1.

The study of electron paramagnetic resonance (EPR) was carried out on E-112 spectrometer (Varian, USA) operating in the X-band at room temperature. The concentration of paramagnetic centers was determined by comparison with the standard, as standard a certified sample of coal powder with a certain concentration of centers was used, the g-factor was determined from the known values of the g-factors of the reference lines in the EPR spectrum of Mn²⁺ ions in MgO powder and direct measurements of the frequency of microwave radiation and the magnitude of the magnetic field strength under resonance conditions.

Light attenuation spectra (LAS) of synthesized glasses were recorded on the Cary-500 spectrophotometer (Varian, USA-Australia), and luminescence spectra (LS) and luminescence excitation spectra (LES) — on the Fluorolog-3 spectrofluorimeter (HORIBA Scientific, USA). A PPD-850 Peltier-cooled photomultiplier (HORIBA Scientific) was used as a detector during LES measurements in the UV

and visible spectral regions, and R5509-73 liquid nitrogen-cooled PMT (Hamamatsu, Japan) was used in the near-IR region of the spectrum. To record LS in the visible region of the spectrum and up to 1050 nm a Peltier-cooled silicon CCD-matrix Sincerity (HORIBA Scientific) was used. The resulting LS and LES were corrected taking into account the spectral sensitivity of the recording system and the distribution of the spectral density of the exciting radiation, respectively, and were expressed as the dependence of the number of quanta per unit wavelength interval ($dN/d\lambda$) on λ .

The luminescence quantum yield (η) was determined by a well-known method using the relation

$$\eta = \eta_{et} S_x A_{et} I_x n_x^2 / S_{et} A_x I_{et} n_{et}^2, \quad (1)$$

where S is area under LS; A is sample absorption in %; I is „quantum“ intensity of excitation light; the indices „ x “ and „ et “ refer to the test sample and standard, respectively. Certified GLS-2 neodymium glass with an absolute luminescence quantum yield of 67% and a refractive index of 1.526 at $\lambda = 589$ nm was used as a standard.

To measure the luminescence decay kinetics, a SpectraLED-390 pulsed LED (HORIBA Scientific) with a radiation wavelength of 389 nm and a pulse duration at half-width of 50 μs was used as an excitation source. Registration was carried out at $\lambda_{reg} = 976$ nm using R5509-73 photomultiplier. The resulting curves were approximated by two exponents in DAS6 program (HORIBA Scientific):

$$F(t) = A + B_1 e^{-t/\tau_1} + B_2 e^{-t/\tau_2}, \quad (2)$$

where the percentage contribution of each of the components (by intensity) was calculated as

$$B_i = B_i / (B_1 + B_2), \quad (3)$$

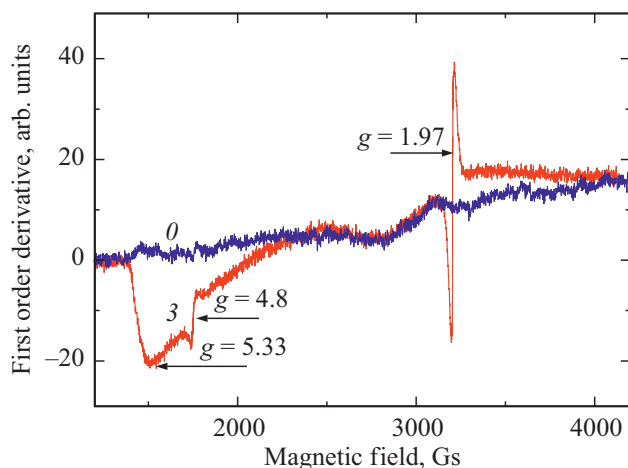


Figure 1. Typical EPR spectra of the studied glasses. Explanations in the text.

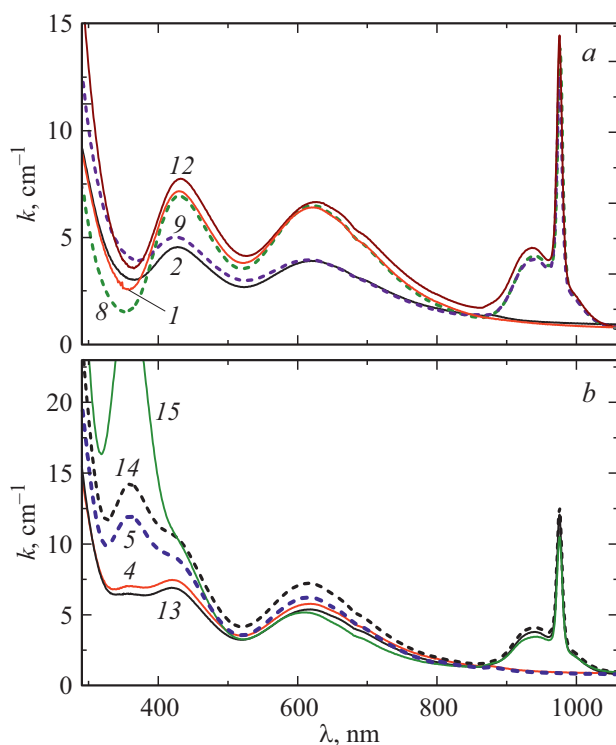


Figure 2. Light attenuation spectra of alkali-free (a) and alkaline (b) glasses. Explanations in the text.

and the average lifetime was determined by the formula

$$\langle \tau \rangle = B_1\tau_1 + B_2\tau_2. \quad (4)$$

Temperature measurements were carried out using a Luma 40S temperature-controlled cell holder (Quantum Northwest, USA) in a quartz cell filled with distilled water. The time interval between measurements ensured the temperature equalization of the cell and the sample.

Results

Figure 1 shows EPR spectra of glass with composition (mol%) $9.5Y_2O_3-0.5Yb_2O_3-30Al_2O_3-60B_2O_3+5Na_2O$ (curve 0) and of sample 3. Here and further, the numbers of the curves correspond to the numbers of the glass samples in the Table 1. It can be seen that Cr-containing glass is characterized by relatively narrow signals at $g \approx 1.97$ and 4.8 and wide signals at $g \approx 5.33$. The listed signals are observed in the spectra of all glasses given in the Table 1, with main difference in relative intensities and spectral width of the signal at $g \approx 4.8$. Experimental values of g -factor, the width (ΔH) and the relative intensity (I) of the signals, as well as the partial concentration of spins (N_i) for glasses with the same concentration of Cr_2O_3 (0.2 mass%) are summarized in the Table 2. As can be seen from this table, the partial replacement of Al_2O_3 by SiO_2 is accompanied by an increase in N_1 and N_2 (compare samples 1 and 3, and 8 and 7), while the value I slightly decreases for glasses without Yb (compare samples 1 and 3) and increases by many times in its presence (compare samples 8 and 7). When B_2O_3 is substituted, this trend is not observed (compare samples 8, 10–12). The substitution of Y for Yb in silica-free glass has little effect on N_1 and N_2 , however, the value I passes through an extremum (compare samples 1, 6, 8), while in silica glass such a substitution is accompanied by a significant N_1 and I increasing with a slight decreasing of N_2 (compare samples 3 and 7). Alkalinization of glasses, in which Al_2O_3 is partially replaced by SiO_2 , is accompanied by N_2 decreasing and N_1 and I passage through the extremum (compare samples 3–5 and 13–15).

Figure 2 shows the LAS of the studied glasses. Here, a number of spectra are omitted due to their almost complete coincidence with those shown: the curve 1 coincides with the curve 3, 6 with 7, 12 with 10 and 11. As can be seen, the spectra of alkali-free Cr-containing glasses contain wide weakly structured bands with maxima at $\lambda_{max} \approx 430$ and 620 nm. The coactivation of these glasses by Yb^{3+} ions is accompanied by the appearance of an additional structural band with $\lambda_{max} \approx 976$ nm. The silica introduction has practically no effect on these spectra. The alkalinization of such glasses is accompanied by the appearance of an additional diffuse band at $\lambda \approx 360$ nm, the intensity of which increases with increasing of Na_2O concentration (compare curves 13, 14, 15), and a noticeable decreasing of the values k in the band with $\lambda_{max} \approx 620$ nm (compare curves 1 and 12 with curves 4, 5 and 14, 15, respectively).

Figure 3 shows the LAS in the region of the long-wavelength wing of the absorption band with $\lambda_{max} \approx 620$ nm of Cr-containing glasses, recorded at a rate of 60 nm/min and a step of 0.1 nm. Here, curve O' belongs to non-activated glass with composition (mol%) $10Y_2O_3-30Al_2O_3-60B_2O_3$. It can be seen that this wing goes at least up to 1400 nm. The silica introduction into alkali-free glass is accompanied by a noticeable k increasing in the region of 1000–1300 nm (compare curves 1 and 3).

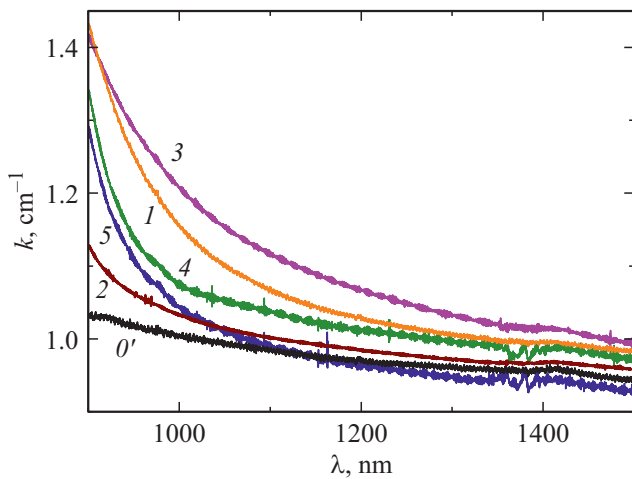


Figure 3. Light attenuation spectra in near-IR region. Explanations in the text.

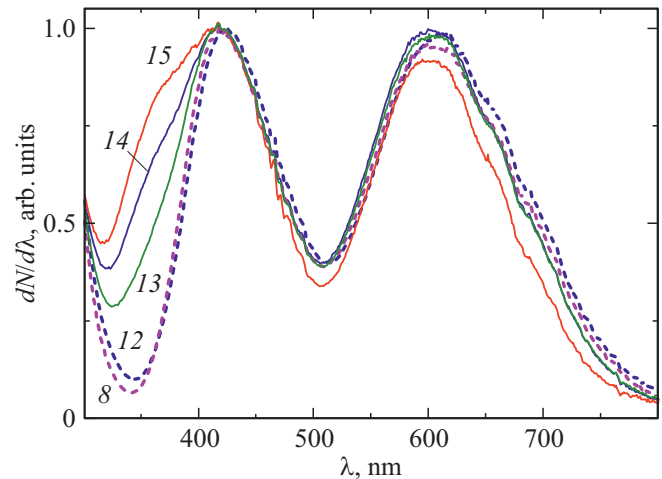


Figure 5. Luminescence excitation spectra. $\lambda_{\text{rec}} = 1010$ nm. Explanations in the text.

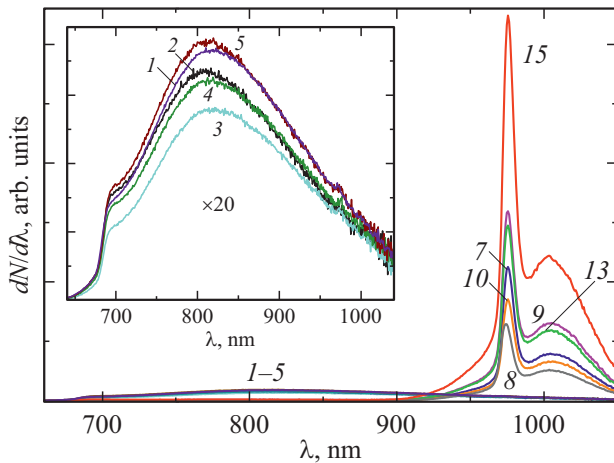


Figure 4. Spectra of luminescence. $\lambda_{\text{exc}} = 600$ nm. Explanations in the text.

A two times decreasing of Cr concentration in such glass leads to a disproportionate decreasing of the IR absorption intensity (compare curves 3 and 2). Additional introduction of Na_2O into such glasses is also accompanied by a significant decreasing of this absorption (compare curves 3–5).

Figure 4 shows the LS reduced to the same number of absorbed quanta at the excitation wavelength $\lambda_{\text{exc}} = 600$ nm. It is seen that LS of Cr-containing glasses characterized by wide band ($\Delta\lambda \approx 230$ nm) with $\lambda_{\text{max}} \approx 810$ nm and embossed shoulder at $\lambda \approx 700$ nm. The relative intensity change of this band depending on the glass composition does not exceed 30% (compare curves 1–5 in the insert). Coactivation of Cr-containing glasses with Yb^{3+} ions results in a multiple weakening of this band and the appearance of a luminescence band of these ions. The minimum intensity of the latter is realized for silica-free glass (curve 8) and increases by about 25% with the introduction of 5 mol% SiO_2 (curve 10). SiO_2 concentration increasing to 15 mol% has practically no effect on the intensity of the integral

luminescence of such glass — curve 12 coincides with the curve 10 within the experimental error and is not shown in the Figure. At the same time, this intensity increases significantly with Na_2O concentration increasing (compare curves 10, 13, 15). Here, attention should be paid to a noticeable increasing of the luminescence intensity of the studied glasses with concentration decreasing of Yb (compare curves 10 and 7) or Cr (compare curves 10 and 9). Note also that there are no additional luminescence bands of these glasses in the near-IR region (1.0–2.0 μm), and at $\lambda_{\text{exc}} = 470$ nm almost by three orders lower intensity of wide band with $\lambda_{\text{max}} \approx 550$ nm is observed.

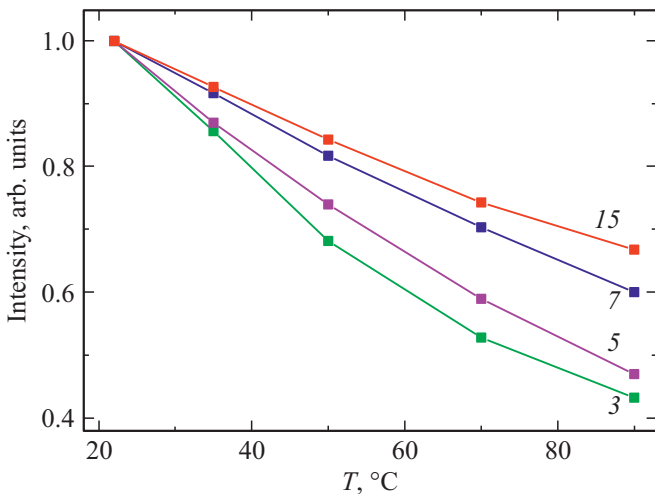
The luminescence quantum yield of sample 15, determined using formula (1) at $\lambda_{\text{exc}} = 585$ nm, was 32%. Using the data in Fig. 4, it is easy to determine that values η for the rest of the samples are as follows: 6.4% (sample 1), 5.8% (2), 4.9% (3), 5.7% (4), 6.6% (5), 11.2% (7), 7.0% (8), 17.0% (9), 8.9% (10–12), 15.6% (13).

Figure 5 shows the LES of Yb^{3+} ions in Cr–Yb-containing glasses, obtained at detection wavelength of $\lambda_{\text{rec}} = 1010$ nm and reduced in maximum to 1. It can be seen that the spectra of alkali-free glasses (samples 6–12) are represented by two wide bands at $\lambda_{\text{max}} \approx 420$ nm and 610 nm with shallow depressions in the long-wavelength band at $\lambda \approx 645$ nm and 680 nm. It should be noted that the spectra of such glasses with different concentrations of SiO_2 (samples 10–12) and Yb_2O_3 (samples 6 and 8) practically coincide, and therefore one curve of each (curves 12 and 8, respectively) are presented. The spectra of alkali glasses are characterized by the appearance of additional branch at $\lambda \approx 360$ nm, the intensity of which varies symbatically with the concentration of Na_2O (see curves 13–15).

The luminescence decay kinetics of Yb^{3+} ions in the studied glasses is non-exponential. The values of the main parameters obtained using formulas (2)–(4) under the conditions described in Section „Experiment“ and characterizing this process are summarized in the Table 3 for a

Table 2. Values of the g -factor, width ΔH and the relative intensity I of the signal, as well as partial concentration of spins N_i

Sample	$g = 1.97$		$g \approx 4.8$		$g \approx 5.33$
	ΔH , Gs	N_1 , 10^{17} spin/g	ΔH , Gs	N_2 , 10^{17} spin/g	I , arb. units
1	35	0.48	40	6.70	1.11
3	35	3.17	60	19.70	1.00
4	35	5.35	50	16.00	1.43
5	35	4.95	45	8.20	1.05
6	35	0.34	40	6.05	1.43
7	35	6.20	55	18.00	1.52
8	35	0.72	50	11.00	0.30
10	35	0.73	50	10.45	0.81
11	35	0.67	40	6.10	0.71
12	35	0.72	50	12.00	0.71
13	35	1.90	60	8.95	0.52
14	35	3.00	50	8.02	0.86
15	35	1.75	40	3.25	0.20

**Figure 6.** Integral luminescence intensity of Cr- and Cr–Yb-containing glasses vs. temperature. $\lambda_{exc} = 600$ nm. Explanations in the text.**Table 3.** Partial durations of exponential stages of luminescence decay (τ_1 , τ_2), relative amplitudes (B_i), average duration ($\langle\tau\rangle$) and Pearson's goodness-of-fit test (χ^2)

Sample	τ_1 , τ_2 , μs	B_1 , B_2	$\langle\tau\rangle$, μs	χ^2
7	151, 325	0.42, 0.58	253	1.04
8	97, 230	0.22, 0.78	206	1.03
9	179, 357	0.31, 0.69	302	1.04
13	135, 287	0.41, 0.59	224	1.06
15	179, 397	0.54, 0.46	279	1.03

number of glasses. Note here that the used approximation of the luminescence decay kinetic curves by two exponentials is formal and allows us to judge only the degree of their non-exponentiality. In this case, a slight deviation of χ^2 criterion from 1 indicates an acceptable accuracy of fitting the calculated curve to the experimental one.

Figure 6 shows the integrated luminescence intensity of a number of glasses versus their temperature. It can be seen that the luminescence intensity of alkali-free Cr-containing glass decreases to the greatest extent with temperature increasing (curve 3). The alkali introduction somewhat reduces the amplitude of such a drop (curve 5). For Cr–Yb-containing glasses, the temperature decreasing in the luminescence intensity is much weaker (compare curves 3 and 5 with curves 7 and 15). Note that for samples 8–14 the experimental values lie within the range limited by curves 7 and 15. For Yb-containing glasses, both alkali-free and alkaline, the luminescence intensity in the studied temperature range decreases by maximum 3%, slightly exceeding the experimental error (2%).

Discussion

According to the publications [16–22], the EPR signal in Fig. 1 at $g \approx 1.97$ can be attributed to Cr^{5+} ions and exchange-coupled pairs of octahedral coordinated ions Cr^{3+} or to isolated Cr^{3+} centers of cubic symmetry, the signal at $g \approx 4.8$ — to isolated Cr^{3+} ions in a highly distorted octahedral environment, and a wide signal at $g \approx 5.33$ is attributed to isolated „octahedral“ Cr^{3+} of rhombic symmetry in a strong local field. It was shown in [13] that the concentration of paired Yb–Yb centers in huntite-like glass is approximately by two orders of magnitude lower than in high-silica gel glass. There are no grounds to assume the formation in the studied glass of noticeable fraction of „cubic“ centers Cr^{3+} . Therefore, the contribution of the latter to the EPR signal at $g \approx 1.97$ can be neglected, taking into account the relatively low concentration of chromium of these exchange-coupled pairs $Cr^{3+}-Cr^{3+}$. Determining the concentration of Cr atoms in these glasses by the formula $N_{Cr} = 0.02N_A P/M$, where N_A , p and M are the Avogadro number, mass% Cr_2O_3 and its molar mass, respectively, we find that it is $\approx 15.84 \cdot 10^{18}$ atom/g. This allows, considering the data in

the Table 2, to estimate the maximum fractions of Cr^{5+} ions and highly distorted $[\text{CrO}_6]^{9-}$ polyhedra in these glasses at the level of 3.9% (sample 7) and 12.4% (sample 3), respectively, of the total chromium concentration. The estimate of the fraction of centers with $g \approx 5.33$ is less unambiguous, since the correct determination of the spin concentration is a problem due to the large width and unusual shape of the EPR signal. Nevertheless, based on the much greater width and intensity of this signal as compared to the close signal with $g \approx 4.8$, it can be stated that for most glasses the fraction of the corresponding centers prevails. The only exception is, perhaps, sample 15, which is characterized by the minimum values of $N_1 + N_2$ and I , indicating the presence of a significant fraction of chromium in the non-paramagnetic form in it. Note that in the absence of strict reducing synthesis conditions only Cr^{4+} and Cr^{6+} [5] can be such ions.

The differences noted in the description of the Table 2 in the nature of the values change N_1 , N_2 and I upon substitution of Al_2O_3 or B_2O_3 by SiO_2 , and also Y_2O_3 by Yb_2O_3 can be associated with the effect on the optical centers of chromium of non-similar changes in the structure of the glass skeleton due to the difference in the energy of affinity for oxygen of aluminum, silicon and boron ($E_{\text{Al-O}} > E_{\text{Si-O}} > E_{\text{B-O}}$) and coordination instability of Yb^{3+} ions [23]. This explanation is also supported by different change of values n . As can be seen from the Table 1, partial substitution of Al_2O_3 or B_2O_3 5 mol% SiO_2 decreases n by 0.008 (compare samples 1 and 3) and 0.0017 (compare samples 8 and 10), respectively, while the substitution of 2 mol% Y_2O_3 by Yb_2O_3 decreases by 0.004 (compare samples 1 and 8).

It is well known that Cr^{3+} ions in oxide glasses are characterized by typical for octahedral centers wide spin-enabled but prohibited by symmetry absorption bands ${}^4A_2 \rightarrow {}^4T_1$ ($\lambda_{\text{max}} \approx 420$ nm) and ${}^4A_2 \rightarrow {}^4T_2$ ($\lambda_{\text{max}} \approx 610$ nm); Cr^{4+} ions (in tetrahedral coordination) — by wide electric dipole absorption band ${}^3A_2 \rightarrow {}^3T_1$ with $\lambda_{\text{max}} \approx 620$ nm, weak magnetic dipole band ${}^3A_2 \rightarrow {}^3T_2$ near 1 μm and more weak absorption in the region longer than 1200 nm, due to Fano antiresonance for transitions ${}^3A_2 \rightarrow {}^1E$ and ${}^3A_2 \rightarrow {}^3T_2$ [24]; Cr^{5+} ions — by wide absorption band at $\lambda_{\text{max}} \approx 465$ nm (in octahedral environment) [25] and bands at $\lambda_{\text{max}} \approx 670$ nm and 1100 nm (in tetrahedral environment) [26], and oxocomplexes $[\text{CrO}_4]^{2-}$ — by charge transfer band $\text{Cr}^{6+}\text{O}^{2-} (3d^0 2p^6) \rightarrow \text{Cr}^{5+}\text{O}^- (3d^1 2p^5)$ at $\lambda_{\text{max}} \approx 360$ nm [25]. Therefore, considering the above mentioned, we can assume that the dominant contribution to the absorption spectra of samples 1–14 in Fig. 2 is made by the bands ${}^4A_2 \rightarrow {}^4T_1$ and ${}^4A_2 \rightarrow {}^4T_2$ of Cr^{3+} ions. In this case, in sample 8, according to the small values I and $N_1 + N_2$ (see Table 2) and the band absence at $\lambda \approx 360$ nm (see Fig. 2, curve 8), a significant fraction of chromium is realized in the form of Cr^{4+} . As for sample 15, then based on 35% intensity decreasing of the band ${}^4A_2 \rightarrow {}^4T_2$, a multiple increasing of the band with $\lambda_{\text{max}} \approx 360$ nm and

minimum values $N_1 + N_2$ and I , the fraction of its non-paramagnetic centers $[\text{CrO}_4]^{2-}$ is comparable to the fraction of Cr^{3+} ions. This situation is also supported by a noticeable (≈ 10 nm) short-wavelength shift of the maximum of „red“ absorption band (Fig. 2, compare curves 1 and 15), indicating the Cr^{4+} fraction decreasing. The presence of the latter, as well as of $[\text{CrO}_4]^{3-}$ polyhedrons in the studied glasses, is confirmed by the IR absorption spectra in Fig. 3, the intensity of which does not contradict the results of the EPR study. Significantly greater degree of absorption decreasing in the near-IR region as compared with the decreasing in the band ${}^4A_2 \rightarrow {}^4T_2$ of Cr^{3+} ions as the glass alkalinizes (compare the corresponding curves in Fig. 3 and Fig. 2) indicates the primary oxidation of Cr^{4+} and Cr^{5+} ions, which can be attributed to the lower stability of $3d$ -electronic configuration of the latter as compared to Cr^{3+} , in which it is half filled. This conclusion contradicts with N_1 increasing in the Table 2 (compare samples 3–5 and 13–15), and is resolved if the fraction of six-coordinated Cr^{5+} ions increases simultaneously. It is worthy of note that with decreasing of the chromium concentration the fraction of Cr^{4+} and Cr^{5+} falls more rapidly (Fig. 3, compare curves 3 and 2).

According to the foregoing, the main contribution to the LS of the studied glasses should be made by Cr^{3+} ions. Therefore, the luminescence of Cr-containing glasses in Fig. 4 (see insert) can be interpreted in the first approximation as a superposition, forbidden by symmetry, but allowed by the band spin ${}^4T_2 \rightarrow {}^4A_2$ ($\lambda_{\text{max}} \approx 820$ nm) and narrow, forbidden by spin and symmetry band ${}^2E \rightarrow {}^4A_2$ ($\lambda_{\text{max}} \approx 694$ nm) of such ions. In fact, LS decomposition of such glasses into individual components reveals two more weak bands with $\lambda_{\text{max}} \approx 730$ and 940 nm, the interpretation of which is planned in a separate paper. It should be noted here that the four-coordinated Cr^{4+} and Cr^{5+} ions in a number of matrices demonstrate rather efficient wideband luminescence with λ_{max} in the region of 1.3–1.5 μm [14,24,26]. The absence of such luminescence in our case can apparently be attributed to the effective energy exchange of the metastable states of these ions to high-frequency vibrations of impurity OH groups and BO_3 groups. As for the band with $\lambda_{\text{max}} \approx 550$ nm, it can be attributed to Cr^{5+} luminescence in an octahedral environment, and the weak intensity can be explained by the excitations transfer to Cr^{3+} , Cr^{4+} and four-coordinated Cr^{5+} ions.

A small ($\approx 18\%$) luminescence intensity decreasing with the concentration increasing of Cr_2O_3 from 0.1 to 0.2 mass% (Fig. 4, compare curves 2 and 3), taking into account the several times smaller fraction of Cr^{4+} and Cr^{5+} in a low-doped sample (Fig. 3, compare curves 2 and 3), indicates a relatively weak concentration quenching of Cr^{3+} luminescence. Note that, according to the publications [27,28], such quenching in a vitreous matrix at concentration of $\text{Cr}_2\text{O}_3 \leq 0.1$ mass% is practically absent. Multiple (from 7 to 13 times) luminescence attenuation of chromium ions when 2 mol% Yb_2O_3 is introduced into Cr–Si-containing

glasses indicates the efficient transfer of excitations to Yb^{3+} ions. In this case, the large difference in the luminescence intensity of the latter (Fig. 4, compare curves 10–15) can be logically related to the different fractions of Cr^{4+} and Cr^{5+} ions, which act as luminescence quenchers (both Cr^{3+} and Yb^{3+}) and internal filters screening the absorption bands of Cr^{3+} ions. Obviously, the small fraction of Cr^{4+} and minor fraction of Cr^{5+} in sample 15 are the reason for the relatively large value of the quantum yield of its sensitized luminescence ($\approx 32\%$). Note that this value, despite on the relatively high concentration of doping OH^- -groups ($k_{OH} \approx 2.72 \text{ cm}^{-1}$), is by 1.5 times higher than for glass $50SiO_2-20Al_2O_3-(30-x-y)CaF_2-xCrF_3-yYbF_3$ [29]. Considering the dependence of Yb^{3+} luminescence quenching probability on the concentration of OH^- -groups [13], it can be predicted that the latter decreasing can noticeably increase η .

Shorter wavelength (by 10–20 nm) position of the band ${}^4A_2 \rightarrow {}^4T_2$ of Cr^{3+} ions and the larger steepness of its long-wavelength wing in LES of the studied glasses (Fig. 5) as compared to the LAS (Fig. 2) can be explained by the influence of the internal filter (Cr^{4+} and Cr^{5+} ions) and weak sensitization of Yb^{3+} luminescence by Cr^{5+} ions in a tetrahedral environment. Appearance in LES of alkaline glasses (Fig. 5, curves 13–15) of explicit shoulder at $\lambda \approx 360 \text{ nm}$ indicates the luminescence sensitization of Yb^{3+} ions through charge transfer band $Cr^{6+}O^{2-}(3d^02p^6) \rightarrow Cr^{5+}O^-(3d^12p^5)$. However, the efficiency of such a process (according to the ratio of intensities for curves 13–15 in LES and LAS) is low. As for weak structure on the long-wavelength wing of band ${}^4A_2 \rightarrow {}^4T_2$ at $\lambda \approx 645$ and 680 nm in LES, also visible in LAS, then it is explained by Fano antiresonance for transitions ${}^4A_2 \rightarrow {}^2E$, 2T_1 and ${}^4A_2 \rightarrow {}^4T_2$ [30].

Non-exponentiality of the attenuation luminescence kinetics of Yb^{3+} ions and substantially smaller values of its average duration for glass samples given in the Table 3 as compared to glass with composition (mol%) $8Y_2O_3-2Yb_2O_3-30Al_2O_3-60B_2O_3$, for which $\langle \tau \rangle \approx 500 \mu s$ [13], confirms quenching of Yb^{3+} luminescence by Cr^{4+} and Cr^{5+} ions. Such quenching is especially effective, as can be seen from this Table, for sample 8, which, even though is characterized by a low k_{OH} (Table 1), but, as indicated above, has a high fraction of Cr^{4+} ions.

Significant temperature quenching of Cr^{3+} ions luminescence (Fig. 6, curves 3 and 5) can be logically explained by probability increasing of tunnel transition from the vibrational sublevels of state 4T_2 to highly excited sublevels of the ground state 4A_2 as they approach the point of intersection of their adiabatic curves. A significant efficiency decreasing of such quenching for Cr–Yb-containing glasses is due to the competitive excitations transfer from Cr^{3+} to Yb^{3+} and weak temperature quenching of the luminescence of the latter. Note that knowledge of the temperature dependence of the luminescence intensity of such glasses is important in terms of their practical use.

Findings

Thus, in the glasses of the system $(Y_{1-x}Yb_x)_2O_3-Al_2O_3-B_2O_3-SiO_2+Cr_2O_3+Na_2O$ in the absence of alkali chromium is realized in the oxidation state Cr(III)–Cr(V) with the predominance of Cr(III). The alkalization of these glasses is accompanied by the formation of Cr^{6+} centers due to the oxidation of chromium ions with a lower charge and, first of all, four-coordinated Cr^{4+} and Cr^{5+} . Partial substitution in the matrix, other things equal, of Al_2O_3 by SiO_2 is accompanied by concentrations increasing of Cr^{5+} and strongly isolated distorted polyhedrons $[CrO_6]^{9-}$, while the concentration of isolated $[CrO_6]^{9-}$ with rhombic symmetry in strong local field decreases slightly in glasses without Yb and significantly increases in its presence. When B_2O_3 is substituted by SiO_2 , no such tendency is observed. The Y substitution by Yb is also accompanied by redistribution of the relative concentrations of optical centers of chromium ions. The main contribution to the luminescence sensitization of Yb^{3+} ions is made by Cr^{3+} ions, while Cr^{4+} and, to a lesser extent, Cr^{5+} ions play the role of the luminescence quencher and internal filter. An additional contribution to Yb^{3+} luminescence is made by its sensitization through the charge transfer band in Cr(VI). Reducing the fraction of Cr^{4+} and Cr^{5+} ions by glass alkalizing, optimizing the concentration of chromium and ytterbium, as well as dehydration can increase the quantum yield of the sensitized luminescence of Yb^{3+} ions noticeably higher the achieved 32%. Cr–Yb-containing glasses are characterized by significantly lower temperature quenching of luminescence than in Cr-containing glasses.

Funding

This work was supported by the Belarusian Republican Foundation for Basic Research (grants № F18R-039 and № F19UZBG-005), the Ministry of Science and Higher Education of Russia (grant FSSM-2020-0003), and the Ministry of Innovative Development of Uzbekistan (grant MRB-AN-2019-2021).

Conflict of interest

The authors declare that they have no conflict of interest.

References

- [1] L.J. Andrews, B.C. McCollum, A. Lempicki. *J. Lumin.*, **24–25**, 877 (1981). DOI: 10.1016/0022-2313(81)90109-5
- [2] N.V. Danil'chuk, S.G. Lunter, Yu.P. Nikolaev, G.T. Petrovsky, Yu.K. Fedorov, V.N. Shapovalov. *DAN SSSR*, **266** (5), 1115 (1982).
- [3] S.G. Lunter, A.G. Murzin, M.N. Tolstoy, Yu.K. Fedorov, V.A. Fromzel'. *Sov. Phys. Sol. State*, **14** (1), 66 (1984).
- [4] W.J. Miniscalco. *J. Lumin.*, **31–32**, 830 (1984). DOI: 10.1016/0022-2313(84)90139-X
- [5] N. Iwamoto, Y. Makino. *J. Non-Cryst. Sol.*, **41** (2), 257 (1980). DOI: 10.1016/0022-3093(80)90171-4

- [6] M.A. Hassan, F. Ahmad, Z.M. Abd El-Fattah. *J. Alloys Compd.*, **750**, 320 (2018). DOI: 10.1016/j.jallcom.2018.03.351
- [7] T. Murata, M. Torisaka, H. Takebe, K. Morinaga. *J. Non-Cryst. Sol.*, **220** (2–3), 139 (1997). DOI: 10.1016/S0022-3093(97)00264-0
- [8] R. Lachheb, A. Herrmann, K. Damak, C. Rüssel, R. Maâlej. *J. Lum.*, **186**, 152 (2017). DOI: 10.1016/j.jlumin.2017.02.030
- [9] G.E. Malashkevich, G.I. Semkova, A.V. Semchenko, P.P. Perhukovich, I.V. Prusova. *JETP Letters*, **88** (11), 740 (2008). DOI: 10.1134/S0021364008230082.
- [10] M. Herren, H. Nishiuchi, M. Morita. *J. Chem. Phys.*, **101**, 4461 (1994). DOI: 10.1063/1.467430
- [11] Sh. Payziyev, Kh. Makhmudov. *J. Ren. Sust. En.*, **8** (1), 015902-1 (2016). DOI: 10.1063/1.4939505
- [12] G.E. Malashkevich, V.N. Sigaev, N.V. Golubev, E.Kh. Mammadzhanova, A.A. Sukhodola, A. Palcari, P.D. Sarkisov, A.N. Shimko. *Mat. Chem. Phys.*, **137** (1), 48 (2012). DOI: 10.1016/j.matchemphys.2012.07.055
- [13] G.E. Malashkevich, V.V. Kouhar, E.V. Pestryakov, V.N. Sigaev, N.V. Golubev, M.Z. Ziyatdinova, A.A. Sukhodola. *Opt. Mat.*, **76**, 253 (2018). DOI: 10.1016/j.optmat.2017.12.042
- [14] W. Streck, P.J. Deren, E. Lukowiak, J. Hanuza, H. Drulis, A. Bednarkiewicz, V. Gaishun. *J. Non-Cryst. Sol.*, **288** (1–3), 56 (2001). DOI: 10.1016/S0022-3093(01)00610-X
- [15] Cz. Koepke, K. Wisniewski, M. Grinberg, F. Rozploch. *J. Phys.: Condens. Matter*, **14** (45), 11553 (2002). DOI: 10.1088/0953-8984/14/45/301
- [16] V.K. Zakharov, D.M. Yudin. *Sov. Phys. Sol. State*, **7**, 1267 (1967).
- [17] A. Srinivasa Rao, J. Lakshmana Rao, R. Ramakrishna Reddy, T.V. Ramakrishna Rao. *Opt. Mat.*, **4** (6), 717 (1995). DOI: 10.1016/0925-3467(95)00040-2
- [18] R.P. Sreekanth Chakradhar, J. Lakshmana Rao, G. Sivaramaiah, N.O. Gopal. *Phys. Stat. Sol. (B)*, **242** (14), 2919 (2005). DOI: 10.1002/pssb.200540100
- [19] T. Lesniewski, B.V. Padlyak, J. Barzowska, S. Mahlik, V.T. Adamiv, Z. Nurgul, M. Grinberg. *Opt. Mat.*, **59**, 120 (2016). DOI: 10.1016/j.optmat.2016.01.008
- [20] M.R. Ahmed, K.Ch. Sekhar, A. Hameed, M.N. Chary, Md. Shareefuddin. *Int. J. Modern Physics B*, **32** (8), 1850095-1 (2018). DOI: 10.1142/S0217979218500959
- [21] C. Lin, J. Liu, L. Han, H. Gui, J. Song, C. Li, T. Liu, A. Lu. *J. Non-Cryst. Sol.*, **500**, 235 (2018). DOI: 10.1016/j.jnoncrysol.2018.08.004
- [22] B. Srinivas, B. Srikantha Chary, Abdul Hameed, M. Narasimha Chary, Md. Shareefuddin. *Opt. Mat.*, **109**, 110329 (2020). DOI: 10.1016/j.optmat.2020.110329
- [23] G.A. Bandurkin, B.F. Dzhurinsky, I.V. Tananaev. *Osobennosti kristalokhimiï soedineniy redkozemel'nykh elementov.* (Nauka, Moskva, 1984) (in Russian).
- [24] X. Feng, S. Tanabe. *Opt. Mat.*, **20** (1), 63 (2002). DOI: 10.1016/S0925-3467(02)00048-4
- [25] Cz. Koepke, K. Wisniewski, M. Grinberg. *J. Alloys Comp.*, **341** (1–2), 19 (2002). DOI: 10.1016/S0925-8388(02)00091-9
- [26] P. Gerner, K. Kramer, H.U. Gudel. *J. Lumin.*, **102–103**, 112 (2003). DOI: 10.1016/S0022-2313(02)00476-3
- [27] L.J. Andrews, A. Lempicki, B.C. McCollum. *J. Chem. Phys.*, **74** (10), 5526 (1981). DOI: 10.1063/1.440915
- [28] I.B. Artsybysheva, S.G. Lunter, N.T. Timofeev, Yu.K. Fedorov. *Fizika i khimiya stekla*, **16**, 625 (1990) (in Russian).
- [29] H. Fu, Sh. Cui, Q. Luo, X. Qiao, X. Fan, X. Zhang. *J. Non-Cryst. Sol.*, **358** (9), 1217 (2012). DOI: 10.1016/j.jnoncrysol.2012.02.024
- [30] A. Lempicki, L. Andrews, S.J. Nettel, B.C. McCollum. *Phys. Rev. Lett.*, **44** (18), 1234 (1980). DOI: 10.1103/PhysRevLett.44.1234